Available online at www.sciencedirect.com

ScienceDirect

Proceedings of the Combustion Institute 37 (2019) 2867–2874

Proceedings of the Combustion Institute

www.elsevier.com/locate/proci

Numerical study of coal particle ignition in air and oxy-atmosphere

Sima Farazi [a,*], Antonio Attili [a], Seongwon Kang [b], Heinz Pitsch [a]

[a] *Institute for Combustion Technology, RWTH Aachen University, Aachen 52056, Germany*
[b] *Department of Mechanical Engineering, Sogang University, Seoul, Republic of Korea*

Received 30 November 2017; accepted 1 July 2018
Available online 30 July 2018

Abstract

The ignition and combustion of coal particles are investigated numerically under conventional and oxy-fuel atmospheres. Devolatilization is computed using the chemical percolation devolatilization (CPD) model. The CPD model is coupled with a Lagrangian particle tracking method in the framework of a multiphysics, multiscale Navier–Stokes solver. Combustion in the gas phase is described using finite rate chemistry. The numerical results for ignition are compared with available experimental data and a remarkably good agreement is observed. The effect on flame ignition of the different phases characterizing the release of volatile gases is assessed. These different phases manifest themselves in two distinct peaks in the devolatilization rate and it is observed that ignition can occur during the first volatile release or on the onset of the second, depending on the particle size and gas temperature. It is found that an increase of ignition delay time in oxy-atmosphere compared to the air case is related to the depletion of radicals that react with the abundant carbon dioxide of the oxy-atmosphere, while the increased heat capacity of the mixture does not play a role.

Keywords: Coal particle; Ignition delay time; Oxy-fuel; CPD

1. Introduction

As coal continues to play a significant role in power generation, oxy-fuel combustion may be a viable technique to capture carbon dioxide, CO_2, and reduce its emissions into the atmosphere [1]. In an oxy-fuel burner, pulverized coal particles burn in an atmosphere in which air is replaced by a mixture of oxygen and recycled exhaust gas, mainly CO_2. Because of the different chemical and thermal properties of N_2 and CO_2, switching from air to oxy-fuel combustion can have significant effects on the ignition and combustion dynamics. Flame stabilization and burner performance under both air and oxy-atmosphere are significantly influenced by the ignition process. Several experimental [2–7] and numerical [8–11] studies indicate that replacing N_2 by CO_2 increases the ignition delay time and duration of devolatilization. Recently, Jimenez and Gonzalo-Tirado [10] simulated coal particle devolatilization

* Corresponding author.
E-mail address: s.farazi@itv.rwth-aachen.de (S. Farazi).

https://doi.org/10.1016/j.proci.2018.07.002
1540-7489

in air and oxy-atmospheres. They explained the longer devolatilization period by the lower peak temperatures observed in the oxy-atmosphere case, which resulted from the combined effect of the chemical properties and the higher heat capacity of CO_2. However, the primary effect of CO_2 on retarding the onset of ignition remains unclear and has been a matter of debate. In the present work, we perform numerical simulations of coal particle ignition using detailed sub-models for the devolatilization process and the chemical reactions in the gas phase. The results in air and oxy-atmosphere are compared and the mechanisms responsible for the increased ignition delay in oxy-atmosphere are investigated and assessed.

For both air and oxy-atmospheres, the volatile flame evolution is computed applying the chemical percolation devolatilization (CPD) model [12], coupled with finite rate chemistry for gas phase reactions. It has been shown that the application of the CPD model reveals a double peak in the time evolution of the release rate of volatile mass, mostly due to the dynamics of tar [13,14]. A double peak profile has also been observed experimentally in the time evolution of species and temperature measurements around burning coal [15–17]. The link between the double peak in the devolatilization rate produced by the CPD model and the double peak in the species measurement has not yet been investigated in detail. In particular, we investigate the effects of the presence of these two phases in the devolatilization process, which is manifested by the appearance of the double peak in the mass release from coal, on the dynamics of ignition for different particle sizes, gas temperature and composition. The differences of these mechanisms in air and oxy-atmosphere are also assessed.

2. Physical models and configuration

We study devolatilization and ignition of single coal particles surrounded by a mixture of hot gaseous species applying an Euler–Lagrange method [19]. In the gas phase, Eulerian equations for conservation of mass, species, momentum, and energy are solved. Particles are modeled within the Lagrangian framework. Assuming a point particle approximation, Lagrangian equations are solved for particle trajectory, velocity, mass, and temperature.

To compute devolatilization rates and volatile composition, the CPD model [12] is applied. The CPD model describes devolatilization according to the coal molecular structure. The model assumes that the coal lattice contains aromatic rings connected by stable and labile bridges. During devolatilization, cleavage between side chains and aromatic rings results in the release of light gases, whereas breaking between aromatic rings forms so-called finite fragments. The finite fragments with lower molecular weight are vaporized as tar, while the heavier fragments remain in the lattice to form metaplast. We compute the light gas composition as a function of time in the CPD model according to the study by Jupudi et al. [20], in which light gases consist of CH_4, CO, H_2O, CO_2, and "other gases". We assumed the "other gases" calculated by CPD to be C_2H_2. Recently, a similar assumption has been applied by Jimenez and Gonzalo-Tirado [10], Hashimoto et al. [21], and Goshayeshi and Sutherland [18]. Following the work done by Goshayeshi and Sutherland [18] and Tufano et al. [9] on ignition of the same coal considered in the present work, C_2H_2 is assumed as tar species. In addition, to assess the effect of this assumption on ignition delay, we computed one of the cases employing C_6H_6 as tar species instead of C_2H_2 and we observed only a marginal difference in ignition delay time. A detailed description of these results is provided in the supplementary material. Chemical reactions in the gas phase are modeled with finite rate chemistry adopting the GRI 3.0 mechanism [22]. Unity Lewis numbers are assumed for all species.

The Euler equations in the gas phase are solved using a semi-implicit finite difference code, with 2nd order in space and time [23]. Equations are advanced in time applying the Crank–Nicolson method along with an iterative predictor–corrector scheme [24]. The domain is discretized using a uniform grid consisting of cubic cells with size dx equal to the particle diameter D_p. A convergence study showed that for $dx < D_p$ the computed ignition delay time does not change. Therefore, we performed all simulations with $dx = D_p$. Using computational cells that are much bigger than the particle size cannot capture the homogeneous ignition of a single coal particle. This would lead to a very dilute mixture and could artificially prevent ignition. Hence, if the cells are large compared with the particle, ignition needs to be described as part of the film model. Furthermore, according to the study by Jimenez and Gonzalo-Tirado [10], the flame front associated with volatile is located at a distance from the particle smaller than $10D_p$.

In the Lagrangian–Eulerian approach, the film model equations are derived according to the assumption of uniform gas field around the particle. Using the gas phase quantities in the small grid cell that contains the particle, might not be consistent with the film model assumptions. To overcome this problem, we applied a filter to provide a smoother gas phase fields as input for the CPD model so that the state of the particle surroundings are evaluated consistently with the film model. The quantities required from the gas phase are averaged within a cube with side length L_f, centered at the particle location. Sensitivity studies showed that the filter length does not have any significant effect on the results.

Table 1
Conditions for all the particle ignition cases considered: particle diameter D_p, initial gas temperature T_g, and gas phase species mole fractions X_i. In all cases, gaseous mixture contains steam with the value of 0.116 and the initial particle temperature is 300 K.

Case	A(1–7)	B(1–6)	C(1–6)	Air (1–15)	Oxy (1–15)
D_p [μm]	55–125	90	90	55–125	55–125
T_g [K]	1320	1200–1670	1200–1670	1175–1500	1175–1500
X_{N_2}[-]	0.464	0.384	0	0.684	0
X_{CO_2}[-]	0.3	0.3	0.684	0	0.684
X_{O_2}[-]	0.12	0.2	0.2	0.2	0.2

The gas and particle phases are fully coupled through source terms in the respective equations. For each quantity, the relevant source term for the gas phase is distributed within a sphere around the particle with a distribution diameter L_d. The distribution coefficient for each cell is computed from a Gaussian function with a characteristic width L_d, centered at the particle, similarly to the approach applied by Apte et al. [25]. Increasing L_d from dx up to $5dx$ (corresponding to a volume of $125dx^3$) changes ignition delay by less than 10% and does not affect the behavior of the CH profile. With bigger values of L_d, the source term is distributed beyond the reaction zone and influences the results significantly. Here, the distribution length L_d is set to $2D_p$.

Two different configurations are used to represent the experimental configuration of Liu et al. [5], where coal particles are introduced into a hot flow through a thin pipe in a carrier gas. The first configuration assumes fast mixing of the carrier stream with the hot gas so that negligible relative velocity is reached quickly. To assess this assumption, additional simulations are performed considering the mixing process. In the first numerical configuration, a single coal particle with the diameter D_p is located at the center of a cube with side length L, which contains gaseous mixture with initial temperature T_g and species mole fraction X_i. We computed a number of different cases changing both the particle and gas phase parameters. All cases are summarized in Table 1. In cases A(1–7), the particle diameter is varied keeping the gas phase properties constant; in cases B(1–6) and C(1–6), the initial gas temperature is changed. In addition, the N_2 species in B(1–6) is replaced by CO_2 in C(1–6). Cases A, B, and C are used for a detailed validation against experimentally measured ignition delay time data by Liu et al. [5]. For the second configuration, two additional cases with different settings based on a 3D inlet–outlet configuration are employed in order to test the simplification of a periodic domain. Furthermore, to perform a comprehensive comparison between air and oxy-atmosphere, coal ignition is computed in additional 30 different cases. These cases are defined in Table 1 as Air(1–15) in $N_2/O_2/H_2O$ and Oxy(1–15) in $CO_2/O_2/H_2O$ mixtures referred to as air and oxy-atmosphere, respectively.

The computed ignition delay time becomes independent of the domain size L for $L > 31D_p$, so a conservative value $L = 61D_p$ is used.

3. Validation against experiment

Since modeling ignition and combustion of coal particles requires a significant number of physical models and simplifying assumptions, a comparison with available experimental measurements [5] and previously published numerical results [18] is presented. In order to compare the results in a consistent way, the ignition delay time τ_{igni} is computed with the same criteria used by Liu et al. [5] and Goshayeshi and Sutherland [18]. In the experiment [5], the ignition delay time is defined as the time at which the CH mass fraction reaches half of its maximum value. We also compute the ignition delay time according to the evolution of the maximum mass fraction of CH radical. An error bar for this computation is defined by the width of an interval from the first sharp increase in $Y_{CH,\,max}$ to the time when $Y_{CH,\,max}$ reaches its peak. In the experiment, particles are injected with a carrier gas from a tube with diameter $D_{tube} = 0.75$ mm, located at the center of the burner inlet. In addition, the hot gas oxidizer (coflow) enters the furnace and rapidly mixes with the carrier gas providing the energy for particle heating.

In the experiment, ignition happens at $50D_{tube}$ from the inlet or above. Assuming rapid mixing and a very low particle slip velocity, the ignition of the coal particle is computed in a periodic cube consisting of stationary gas with the same initial composition and temperature as the coflow of the experiment. Uncertainties regarding these assumptions are discussed in the following paragraphs.

Ignition delay time is computed for a large set of conditions, varying particle size (55–125 μm), initial gas temperature (1200–1670 K), and diluent in the gas phase (N_2 and CO_2). We consider 19 cases, labelled as A(1–7), B(1–6), and C(1–6) in Table 1. Figure 1 also shows the ignition delay times for various particle diameters (55–125 μm). This plot includes results from the current study compared with those from the numerical study by Goshayeshi and Sutherland [18] together with experimental data by Liu et al. [5]. Our results are in

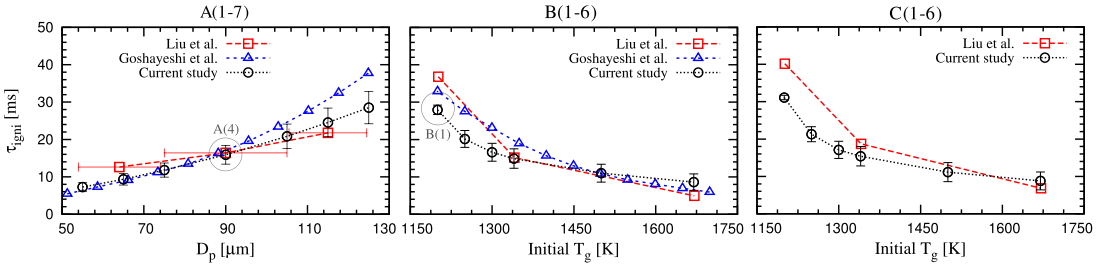

Fig. 1. Ignition delay times at various particle diameters in cases A(1–7), and at various initial gas temperatures in cases B(1–6) and C(1–6). These cases are defined in Table 1. Results from the Current study are compared with experimental data reported by Liu et al. [5] and numerical data by Goshayeshi and Sutherland [18].

good agreement with both numerical and experimental studies. Figure 1 shows the ignition delay time for different values of the initial gas temperature (1200–1670 K). The present results agree well with the numerical simulations of Goshayeshi and Sutherland [18] and with experimental data. Furthermore, we consider the cases C(1–6) with CO_2 as diluent. Also for these cases, the present results are in close agreement with the experimental measurements.

To quantify uncertainties due to the numerical approach and the approximation in the configuration setting, particle ignition is computed in two additional cases. An inlet–outlet set-up, similar to the experiment by Liu et al. [5], is used. For the first case, a single coal particle is injected from the inlet boundary with a jet of carrier gas that differs in terms of gas composition, temperature, and velocity from the surrounding coflow. For the second case, rapid mixing between carrier gas and coflow is assumed, and the particle is injected with the carrier gas having the same composition, temperature, and velocity as the coflow. The second case is very similar to the configuration used by Goshayeshi and Sutherland [18].

The computed ignition delay time in the first case is 9% higher than the one of the fixed particle in a box (case A(4)). This extra time is required for mixing between the carrier stream and the ambient gas inside the burner. Because of the very low particle Reynolds number, ignition delay in the second case is only 1% higher than the one computed for the particle in the periodic box, i.e., case A(4).

4. Volatile flame evolution

The ignition and development of a typical volatile flame is shown in Fig. 2 for the case A(4). The particle diameter considered is $D_p = 90\,\mu m$ and the initial gas temperature is $T_g = 1320$ K. The properties of the hot ambient gas are defined in Table 1. The flame front initially forms in the vicinity of the particle and then moves outwards. At $t = 16$ ms, the flame weakens and moves slightly towards the particle. A decrease in the temperature and the OH mass fraction are observed during this phase. As time progresses, the temperature and radical mass fractions increase again and remain rather stable for a few milliseconds. After $t = 22$ ms, the volatile flame begins to extinguish.

To understand the process of volatile flame formation, the evolution of selected quantities are shown in Fig. 3 for the two different cases A(4) and B(1). These two cases differ in the initial temperature and oxygen concentration in the gas phase. The two cases are compared as they show a different mechanism for the ignition of gas phase reactions. The volatile flame evolves faster in the A(4) case, due to the higher initial gas temperature. In both cases, the particle temperature increases due to the energy transfer from the surrounding gas. Approaching a certain particle temperature, enough bounds inside the coal network break and volatile gases begin to be released from the particle. The released volatiles diffuse away from the particle towards the hot oxidizer and form a volatile flame. The heat released from the volatile flame rapidly increases the gas phase temperature. The elevated temperature of the surrounding gas accelerates particle heating and consequently the devolatilization process is enhanced.

Within the early stage of devolatilization, the rate of devolatilization m_{vol} shows two distinct peaks. This typical behavior is explained by Yang et al. [13] in the context of the CPD model. The first peak is due to the release of light tar compounds not initially connected with the coal lattice. The second peak is caused by the release of heavier tar compounds due to the cleavage of the bridges between aromatic clusters. For the case A(4), the double peak in the devolatilization rate m_{vol} results in two distinct peaks also in the maximum gas temperature $T_{g,max}$. On the contrary, the double peak profile is not present in the gas temperature profile for the case B(1). Because of the lower initial gas temperature of case B(1), the particle does not ignite when the first part of the volatiles is released and ignition occurs only at the onset of the second peak of the devolatilization rate m_{vol}. This is

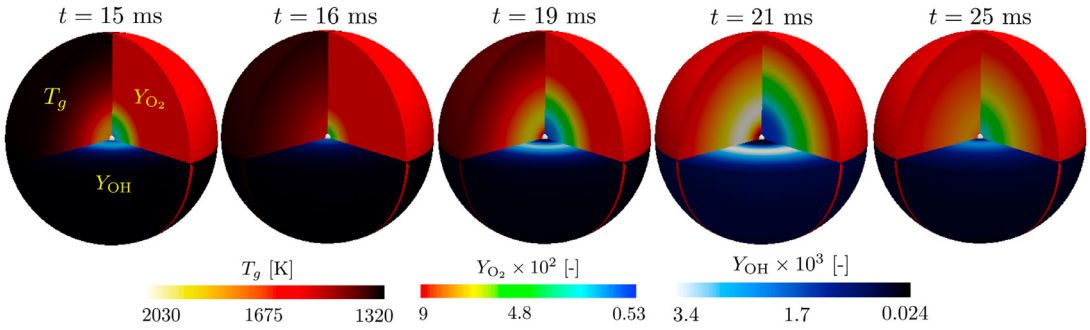

Fig. 2. Distribution of gas temperature, mass fraction of O_2 and OH around the coal particle from time $t = 14$ to 25 ms for case A(4) defined in Table 1 with particle diameter $D_p = 90$ μm.

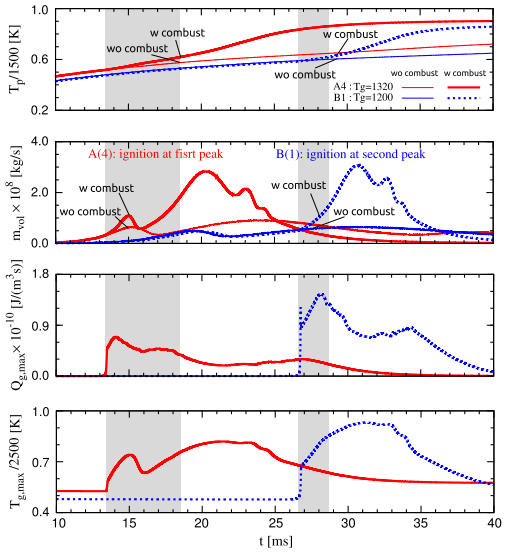

Fig. 3. Evolution of the particle temperature T_p, rate of volatile release m_{vol}, maximum heat release rate from combustion in the gas phase $Q_{g,\,max}$, and maximum temperature of the gas phase $T_{g,\,max}$ for case studies A(4) and B(1). In both cases, particle diameter is 90 μm. Case A(4) has initial gas temperature of 1320 K and oxygen mole fraction of 0.12, while in case B(1), initial temperature is 1200 K and oxygen mole fraction 0.2.

evident from the profile of heat released from gas-phase combustion Q_g, which is negligible for the entire duration of the first volatile release. It is worth noting that the much longer ignition delay time observed for case B(1) compared to A(4) case is mostly related to the lack of ignition during the first release of volatile matter. If ignition happened during the first volatile release also for case B(1), the ignition delay time would be much shorter and close to the value obtained for case A(4). In addition, it is clear that ignition cannot be predicted solely from the devolatilization rate, but the diffusive-reactive processes in the gas phase need to be included.

In order to provide more details on the role of the gas phase flame on the process, the results are compared with two cases at the same conditions and for which the gas phase combustion is artificially suppressed (shown as "wo combust" in Fig. 3. The double peak behavior in the devolatilization rate is still present, proving that it is due to the devolatilization process modeled with the CPD approach. However, the heat release from gas phase combustion significantly increases the maximum value of the second peak and shifts its appearance to a slightly earlier time.

Since the ignition delay time is strongly influenced by the presence (or lack) of significant heat release during the first peak of the devolatilization rate, it is of interest to assess the influence of the particle size and ambient conditions on this phenomenon. From the analysis of the multiple cases described in Table 1, it is found that the particle diameter and the initial gas temperature have strong influence on this process. The abundance of CO_2 is also important, and its effect is described in Section 5. Figure 4 shows the evolution of $T_{g,\,max}$ for several cases with various particle sizes at the same initial gas temperature and cases with different initial gas temperatures for the same particle size. The parametric study reveals that the maximum temperature in the gas phase $T_{g,\,max}$ approaches a double peak profile by increasing the initial gas temperature, the particle size or both. The double peak in the gas phase temperature is observed if ignition occurs during the first peak of devolatilization. The higher initial gas temperature provides more energy to activate gas phase reactions such that the particle can ignite during the first peak of volatile release. The larger particle releases more volatile due to the higher surface area and therefore, enables the ignition at the first peak of volatile release. Figure 4 further shows that the double peak in the flame temperature profile might be present for cases with short and long ignition delay time. Furthermore, we observe that the distance between the two peaks increases if we increase the diameter of the particle or if we decrease the

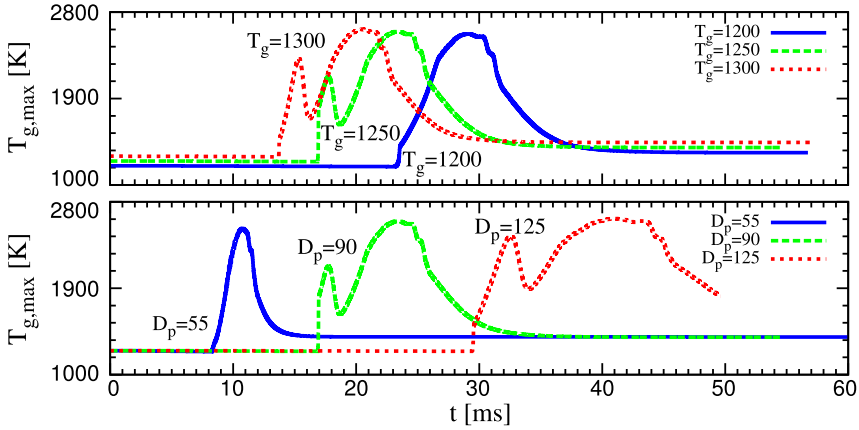

Fig. 4. Evolution of maximum gas temperature for different cases; varying initial gas temperature (with $D_p = 90\,\mu m$) and varying particle size (with initial $T_g = 1250$ K). These cases are defined as air in Table 1.

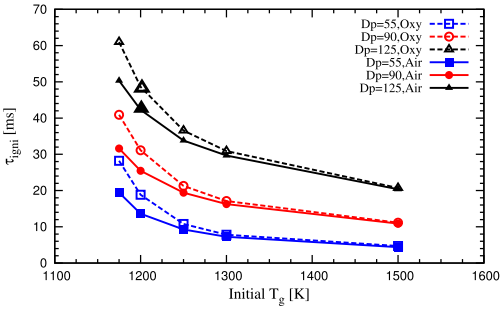

Fig. 5. Ignition delay time for various particle diameters and gas phase temperatures in air and oxy-atmosphere. These cases are defined as Air(1–15) and Oxy(1–15) in Table 1.

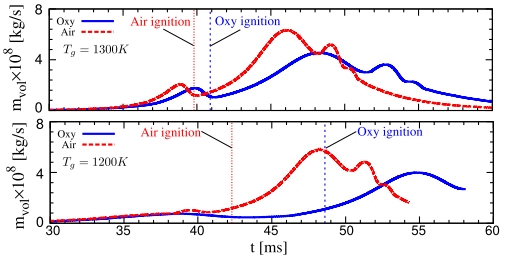

Fig. 6. Evolution of the devolatilization rate for a 125 μm particle in air and oxy-atmosphere with initial temperature $T_g = 1300$ K and $T_g = 1200$ K. Gas composition of air and oxy-atmosphere are defined in Table 1.

initial gas temperature. This analysis might also help to explain the two peaks observed in some experimental measurements of the gas phase temperature and species concentration during coal ignition and combustion [15–17].

5. Coal ignition in air versus oxy-atmosphere

Figure 5 shows the ignition delay time for the air and the oxy-atmosphere at various particle sizes and gas temperatures. Keeping the initial gas temperature constant, ignition delay times decrease with the particle size. Smaller particles ignite faster because they have a higher surface to volume ratio and consequently, heat up faster. For constant particle size, coal particles ignite faster at higher initial gas temperatures. Higher gas temperatures accelerate the devolatilization process as well as the chemical reactions in the gas phase. At lower temperatures and in both atmospheres, the ignition delay time becomes more sensitive to the variation of the initial gas temperature. For all gas temperatures and diameters, coal particles require a longer time to ignite in oxy-atmosphere compared to air. For each particle size, the difference between air and oxy-atmosphere becomes more significant with decreasing initial temperature of the gas phase. To understand the reason of this increased difference, the time evolution of the devolatilization rate for both air and oxy cases at two different temperatures is shown in Fig. 6. For $T_g = 1300$ K, coal particles ignite around the first peak of devolatilization for both atmospheres. For $T_g = 1200$ K, ignition occurs at the onset of the second peak of devolatilization. While the location of the first peak does not change much if the temperature goes from 1300 K to 1200 K, the location of the second peak is much more sensitive to temperature variations.

The slower ignition in oxy-atmosphere can be related to the thermal or chemical effects induced by the presence of CO_2. An increase of ignition delay in the presence of CO_2 was already observed in a number of experiments [2–7], and was ascribed to the higher heat capacity of CO_2, its chemical

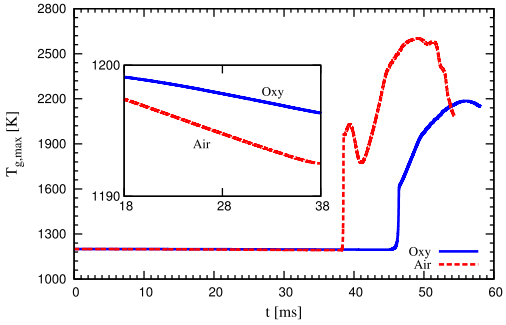

Fig. 7. Evolution of the maximum gas temperature for a 125 μm particle in air and oxy-atmosphere with the initial temperature $T_g = 1200$ K.

properties, or a combination of both. To investigate the reason of the increased ignition delay, we performed a detailed analysis of air and oxy cases with initial gas temperature of 1200 K.

Figure 7 shows the evolution of the maximum gas temperature $T_{g,\,max}$ in both atmospheres. As the coal particle ignites earlier in air atmosphere, the first sharp increase in $T_{g,\,max}$ occurs earlier around $t = 38$ ms. Notwithstanding the earlier ignition in air atmosphere, the zoomed view in Fig. 7 shows that, up to $t < 38$ ms, the oxy-atmosphere case displays a higher temperature in comparison to the air case. This difference can be explained by the heat capacity of CO_2, which is almost 1.5 times higher than the heat capacity of N_2. During particle heating, for the same amount of energy transfer to the particle, the gas phase in the oxy-atmosphere case experiences a smaller temperature drop due to the higher heat capacity of CO_2. Based on this observation regarding the gas temperature in the two cases, we conclude that the higher heat capacity of CO_2 has very little effect on the ignition delay and its effect would be toward a decrease, if any. However, after the occurrence of ignition, the higher heat capacity of CO_2 together with its chemical effect results in lower flame temperature in oxy- compared to air atmosphere, consistently with the analysis by Jimenez and Gonzalo-Tirado [10].

Figure 8 shows the evolution of the maximum value of mass fractions of $Y_{H,\,max}$ $Y_{O,\,max}$, and $Y_{OH,\,max}$ in both atmospheres. As coal ignites earlier in air atmosphere, each radical profile shows the sharp increase in air (around $t = 38$ ms) earlier than in oxy-atmosphere. Also before ignition, the radical mass fractions are higher in air atmosphere. Among all radicals, the early difference in $Y_{H,\,max}$ is most evident. To assess the effect of the presence of CO_2 in the chemistry of ignition, a reaction pathway analysis has been performed. It is found that in oxy-atmosphere, H radicals are strongly consumed by the reaction $R : CO_2 + H \rightarrow CO + OH$. Figure 9 shows the spatial distribution of the rate of this reaction, W_R, at $t = 18, 23,$ and 28 ms. In

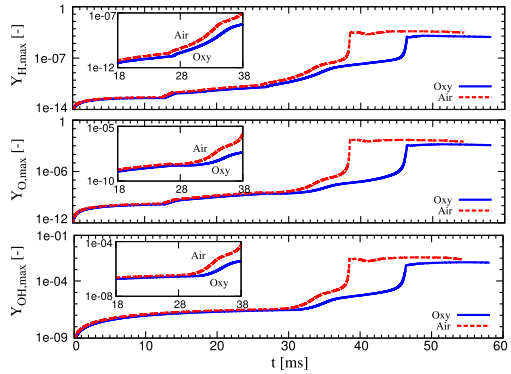

Fig. 8. Evolution of H, O, and OH radical mass fractions for a 125 μm particle in air and oxy-atmosphere with initial temperature $T_g = 1200$ K.

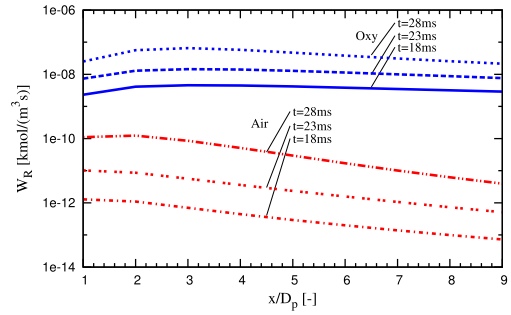

Fig. 9. Distribution of reaction rate W_R for a 125 μm particle in air and oxy-atmosphere with initial temperature $T_g = 1200$ K.

comparison to air atmosphere, W_R is almost 1000 times higher in oxy-atmosphere. The reaction rate W_R depends on the gas temperature and the concentrations of H and CO_2 species. In oxy-atmosphere, the rate of reaction is much higher due to the higher CO_2 concentration. In fact, the higher concentration of CO_2 causes an almost complete depletion of H radicals. H radical depletion decelerates intermediate reactions that are responsible for the production of O and OH radicals such as $O_2 + H \rightarrow OH + O$ and, consequently, O and OH mass fractions are reduced. We conclude that the presence of CO_2 decreases the reactivity of the mixture by reducing the mass fraction of radicals (primarily H and consequently O and OH), which results in delayed ignition.

6. Conclusions

A large set of numerical simulations based on detailed sub-models for the description of coal particle ignition in a hot gas atmosphere has been performed. The numerical results are validated

against a series of experiments in a laminar entrained flow reactor.

The evolution of the volatile flame, resulting from the ignition of the volatile gas released by the particle, is described. A double peek profile in the time evolution of tar release rate is observed and the effect on the gas phase combustion is assessed. It is found that ignition can be strongly influenced by the present of the two distinct peaks. In particular, it is observed that ignition occur in correspondence of the first peak of the devolatilization rate for high gas temperature and large particles, whereas it is delayed until the second peak for low values of the gas temperature and small particles. If ignition occur during the first devolatilization peak, two distinct peaks are also observed in the evolution of the maximum gas phase temperature and species concentration.

Coal ignition in mixtures with significant amounts of CO_2 diluent is slower compared to the case in standard air environment. It is found that this difference is more significant approaching lower initial gas temperature and that the primary effect of CO_2 on ignition originates from its tendency to suppress radical formation.

Acknowledgments

The authors kindly acknowledge financial support through Deutsche Forschungsgemeinschaft (DFG) through SFB/TRR 129. Computations were performed with computing resources granted by JARA-HPC from RWTH Aachen University under project jara0139 and JUQUEEN [26] at Forschungszentrum Jülich under project JHPC48.

Supplementary material

Supplementary material associated with this article can be found, in the online version, at doi:10.1016/j.proci.2018.07.002.

References

[1] L. Chen, S.Z. Yong, A.F. Ghoniem, *Prog. Energy Combust. Sci.* 38 (2012) 156–214.
[2] A. Molina, C.R. Shaddix, *Proc. Combust. Inst.* 31 II (2007) 1905–1912.
[3] P.A. Bejarano, Y.A. Levendis, *Combust. Flame* 153 (2008) 270–287.
[4] C.R. Shaddix, A. Molina, *Proc. Combust. Inst.* 32 (2009) 2091–2098.
[5] Y. Liu, M. Geier, A. Molina, C.R. Shaddix, *Int. J. Greenhouse Gas Control* 5 (2011) S36–S46.
[6] R. Khatami, C. Stivers, Y.A. Levendis, *Combust. Flame* 159 (2012) 3554–3568.
[7] J. Riaza, R. Khatami, Y.A. Levendis, et al., *Combust. Flame* 161 (2014) 1096–1108.
[8] T. Maffei, R. Khatami, S. Pierucci, T. Faravelli, E. Ranzi, Y.A. Levendis, *Combust. Flame* 160 (11) (2013) 2559–2572.
[9] G.L. Tufano, O.T. Stein, A. Kronenburg, et al., *Fuel* 186 (2016) 285–292.
[10] S. Jimenez, C. Gonzalo-Tirado, *Combust. Flame* 176 (2017) 94–103.
[11] M. Muto, K. Yuasa, R. Kurose, *Fuel* 190 (2017) 136–144.
[12] D.M. Grant, R.J. Pugmire, T.H. Fletcher, A.R. Kerstein, *Energy Fuels* 3 (1989) 175–186.
[13] H. Yang, S. Li, T.H. Fletcher, M. Dong, W. Zhou, *Energy Fuels* 28 (2014) 3511–3518.
[14] K. Luo, J. Xing, Y. Bai, J. Fan, *Energy Fuels* 31 (2017) 6525–6540.
[15] Y. Chen, S. Mori, W.-P. Pan, *Thermochim. Acta* 275 (1996) 149–158.
[16] H. Song, G. Liu, J. Wu, *Energy Convers. Manag.* 126 (2016) 1037–1046.
[17] D. Magalhes, F. Kazan, A. Ferreira, M. Rabaal, M. Costa, *Fuel* 207 (2017) 154–164.
[18] B. Goshayeshi, J. Sutherland, *Combust. Flame* 161 (2014) 1900–1910.
[19] R.S. Miller, J. Bellan, *Phys. Fluids* 12 (2000) 650–671.
[20] R.S. Jupudi, V. Zamansky, T.H. Fletcher, *Energy Fuels* 23 (2009) 3063–3067.
[21] N. Hashimoto, R. Kurose, S.M. Hwang, H. Tsuji, H. Shirai, *Combust. Flame* 159 (2012) 353–366.
[22] G.P. Smith, et al. GRI 3.0, accessed, May 2017, (available at http://www.gaseq.co.uk/).
[23] O. Desjardins, G. Blanquart, G. Balarac, H. Pitsch, *J. Comput. Phys.* 227 (2008) 7125–7159.
[24] S. Farazi, M. Sadr, S. Kang, et al., *Fuel* 201 (2017) 15–28.
[25] K. Mahesh, T. Lundgren, *Int. J. Multiph. Flow* 34 (2008) 260–271.
[26] Jülich Supercomputing Centre, *Journal of Large-scale Research Facilities* 1 (2015).